Title: Photoperiodic control of seasonal growth is mediated by ABA acting on cell-cell communication

Authors: S. Tylewicz[1,†], A. Petterle[1], S. Marttila[2], P. Miskolczi[1], A. Azeez[1,3], R. K. Singh[1], J. Immanen[4], N. Mähler[5], T. R. Hvidsten[5,6], D. M. Eklund[7], J. L. Bowman[8], Y. Helariutta[9], R. P. Bhalerao[1,*]

Affiliations:

[1]Umeå Plant Science Centre, Department of Forest Genetics and Plant Physiology, Swedish University of Agricultural Sciences, SE-901 87 Umeå, Sweden

[2]Department of Plant Protection Biology, Swedish University of Agricultural Sciences, Box 102, SE-230 53 Alnarp, Sweden

[3]Plant Molecular Biology Lab, Jain R&D Lab, Agri Park, Jain Hills, Shirsoli Road, Jalgaon, India

[4]Department of Biosciences, Institute of Biotechnology, University of Helsinki, Viikinkaari 1 (P.O.Box 65), Helsinki, Finland

[5]Umea Plant Science Centre, Department of Plant Physiology, Umeå University, SE-901 87, Umeå, Sweden

[6]Faculty of Chemistry, Biotechnology and Food Science, Norwegian University of Life Sciences, Ås, Norway

[7]Department of Plant Ecology and Evolution, Evolutionary Biology Centre, Uppsala University, SE-75236 Uppsala, Sweden

[8]School of Biological Sciences, Monash University, Melbourne, VIC, Australia

[9]Sainsbury Laboratory, Cambridge University, Bateman Street, Cambridge, United Kingdom

*Corresponding author. Email: rishi.bhalerao@slu.se

†Present address: Department of Plant and Microbial Biology, University of Zürich, Zollikerstrasse 107, 8008 Zürich, Switzerland

Abstract: In temperate and boreal ecosystems, seasonal cycles of growth and dormancy allow perennial plants to adapt to winter conditions. We show, in hybrid aspen trees, that photoperiodic regulation of dormancy is mechanistically distinct from autumnal growth cessation. Dormancy sets in when symplastic inter-cellular communication through plasmodesmata is blocked by a process dependent upon the phytohormone abscisic acid (ABA). The communication blockage prevents growth-promoting signals from accessing the meristem. Thus, precocious growth is

disallowed during dormancy. The dormant period, which supports robust survival of the aspen tree in winter, is due to loss of access to growth promoting signals.

One Sentence Summary: Photoperiodic signals transduced via plant hormone abscisic acid enables winter survival by dormancy establishment in trees

Main Text:

Dormancy protects meristematic cells of perennial plants in temperate and boreal ecosystems by preventing growth during winter. Release from dormancy enables reinitiation of growth when favorable conditions return in spring *(1)*. Shorter photoperiods as winter approaches *(2)* induce growth cessation, formation of a bud enclosing the arrested leaf primordia and shoot apical meristem (SAM) (Fig. 1A), and bud dormancy *(3, 4)*. Longer photoperiods alone cannot promote growth in dormant buds; prolonged exposure to low temperatures is required to release dormancy *(5, 6)*. We show that blockage of symplastic communication mediated by the action of abscisic acid (ABA) is part of the photoperiodically controlled dormancy mechanism in hybrid aspen.

Short photoperiods induce expression of ABA receptors and increase ABA levels in hybrid aspen buds *(4, 7)*. ABA regulates dormancy *(8)*. Therefore, we probed ABA's role in photoperiodic control of bud dormancy. First, we generated hybrid aspen plants with reduced ABA responses by expressing the dominant negative *abi1-1* allele of *ABI1*, a key ABA-signaling gene *(9)*. Those hybrid aspens that expressed *abi1-1* had reduced ABA responses, manifested by weak induction of the ABA-inducible gene *KIN2*, compared to wild-type (WT) controls (Fig. S1). We then assessed bud dormancy by exposing WT and *abi1-1* plants to 11 weeks of short photoperiod followed by transfer to long photoperiod without low temperature treatment required for dormancy release. Both WT and *abi1-1* plants ceased growth and set buds after 4

weeks of short photoperiod (Fig 1A-C), but after 11 weeks of short photoperiod followed by long photoperiod, WT buds remained dormant, whereas *abi1-1* buds reactivated growth within 11-15 days (Fig. 1D-F). Thus, attenuation of ABA responses compromised photoperiodic control of bud dormancy and not growth cessation.

We investigated transcriptomic responses to short photoperiod in WT and *abi1-1* apices to understand ABA mediated control of dormancy. After 6 and 10 weeks of short photoperiod, respectively, we detected: 9290 and 3053 differentially expressed genes in WT and 10514 and 2149 in *abi1-1* (line 1) apices (Table S1). A large number of transcripts for plasmodesmata associated proteins responded to short photoperiod. Plasmodesmata closure (by callosic dormancy sphincters) correlates with dormancy and their opening with dormancy release in diverse plants, including hybrid aspen and charophycean algae such as Chara *(6, 10, 11)*. Of 187 poplar homologs of Arabidopsis genes encoding proteins enriched in plasmodesmata *(12)*, 62 and 47 were induced after 6 and 10 weeks in WT apices, respectively, and of these 53.2 and 76.6% were differentially expressed in *abi1-1* relative to WT apices at these time-points (Table S2). Expression of *GERMIN-LIKE 10*, *REMORIN-LIKE 1* and *2*, implicated in plasmodesmata function *(13)*, and *CALLOSE SYNTHASE 1*, required for callose deposition *(6)*, was progressively upregulated, while that of *GH17-39*, a glucanase implicated in sphincter removal *(6)*, was downregulated in WT apices after 6 and 10 weeks of short photoperiod. These genes showed altered response to short photoperiod in *abi1-1* plants (Fig. S2). Thus, ABA mediates short photoperiod response of plasmodesmata-related transcriptome.

Transcriptomic analysis prompted us to investigate ABAs' role in plasmodesmata closure (Fig 1 G-O). Under long photoperiod, WT and *abi1-1* lines 1 and 3 had similar frequencies of 'closed' plasmodesmata with dormancy sphincters (12.5 versus 17.4 and 13.5%, respectively). After 5

weeks of short photoperiod, corresponding frequencies were 78% in WT and 5.5 and 17.4% in *abi1-1* apices, respectively, and after 10 weeks frequencies increased to 83.6% in WT plants, but fell to 2.2 and 0.5% in *abi1-1* lines 1 and 3, respectively. Thus, ABA mediates plasmodesmata closure in response to short photoperiod. Plasmodesmata closure is not required for growth cessation (as growth cessation occurs in *abi1-1* plants) and indicates association of plasmodesmata closure with bud dormancy, both being mediated by the same factor, ABA.

To investigate ABA-mediated plasmodesmata closure's role in short photoperiod-induced dormancy, we over-expressed PDLP1, which impairs trafficking via plasmodesmata *(14)* and phenocopying plasmodesmata blockage by dormancy sphincters, in *abi1-1* plants (Fig. S3). Both *abi1-1/PDLP1* double transformants and parental *abi1-1* plants ceased growth and formed buds under short photoperiod (Fig. 2A-C), but subsequent exposure to long photoperiod only reactivated growth in the latter (Fig. 2D-F). Thus, PDLP1 expression suppressed *abi1-1* plants' bud dormancy phenotype, although, *KIN2* expression responses to ABA remained attenuated in *abi1-1/PDLP1* (Fig. S4). Thus, expression of PDLP1 was sufficient to restore bud dormancy in *abi1-1/PDLP1* plants without the restoration of general ABA responses.

PICKLE (PKL) is an antagonist of polycomb repression complex 2, implicated in seed dormancy *(15, 16)*. *PKL* expression was downregulated in WT plants but upregulated in *abi1-1* plants under short photoperiod (Fig. S5). Hence we investigated whether *PKL* could be involved in plasmodesmata closure and dormancy regulation mediated by ABA. Thus, we examined plasmodesmata in *abi1-1* plants with suppressed *PKL* activity (*abi1-1/PKL*RNAi) (Fig. S6). Under long photoperiod, frequencies of plasmodesmata with dormancy sphincters were comparable in *abi1-1* (13.1%) and *abi1-1/PKL*RNAi lines 9 (19.4%) and 11 (18.4%) (Fig. 3A-C). After 5 weeks of short photoperiod, the frequencies increased in the *abi1-1/PKL*RNAi lines

(to 34.4% and 28.5%, respectively), but not *abi1-1* plants (16.4%) (Fig. 3D-F). After 10 weeks of short photoperiod, the frequencies further increased in *abi1-1/PKL*RNAi lines 9 and 11 to 84.6% and 74.5%, respectively, but fell in *abi1-1* plants (5.2%) (Fig. 3G-I). *PKL* downregulation in *abi1-1/PKL*RNAi also suppressed expression defects of plasmodesmata markers evident in *abi1-1* plants (Fig. S7). While both *abi1-1* and *abi1-1/PKL*RNAi plants ceased growth and set buds (Fig. 3J-L), *abi1-1/PKL*RNAi buds remained dormant and did not reactivate growth (unlike non-dormant *abi1-1* buds) after long photoperiod exposure following 11 weeks of short photoperiod (Fig. 3M-O). Thus, *PKL* downregulation restores plasmodesmata closure and bud dormancy defects in *abi1-1* plants, suggesting that ABA mediates plasmodesmata closure and bud dormancy by suppressing *PKL*.

Plasmodesmata closure could mediate dormancy by limiting access of SAM to growth promotive signals. We investigated this hypothesis by analyzing responses of WT and *abi1-1* buds to *FLOWERING LOCUS T 1* (*FT1*), a seasonal growth regulator induced during dormancy release and before bud growth resumes *(6, 17)*. We grafted scions of WT and *abi1-1* plants exposed to 10 weeks of short photoperiod (to induce plasmodesmata closure and dormancy) onto rootstocks of *FT1*-expressing plants *(18)*. Although buds of WT scions did not reactivate growth, new leaves emerged from buds of *abi1-1* scions under continued short photoperiod (Fig. 4). Thus, plasmodesmata closure, as in WT plants, was associated with buds' failure to respond to FT1 or FT1-derived growth promotive signals, corroborating the involvement of plasmodesmata in photoperiodic control of ABA-mediated bud dormancy.

Thus short photoperiods suppressed FT, which causes growth cessation, and amplifies the ABA response by enhancing levels of ABA and ABA receptors *(4, 7)*. ABA suppresses PKL and induces callose synthase to block plasmodesmata and maintains these blockages by repressing

antagonistic glucanases (Fig. S8). Hence, attenuating ABA responses not only results in a failure to induce plasmodesmata closure at dormancy onset, but also in fewer subsequently closed plasmodesmata. Plasmodesmata closure by *PKL* downregulation or *PDLP1* expression, which both target cell-cell communication, suppresses dormancy defects in *abi1-1* plants. *PDLP1* expression restores dormancy without suppressing ABA response defects in *abi1-1* plants. Thus, plasmodesmata closure is essential to dormancy and occurs downstream of ABA-mediated control of dormancy in response to shorter photoperiods.

With plasmodesmata closed, growth arrest is maintained even in the presence of growth promoting signals. Re-opening of closed plasmodesmata in dormant buds occurs slowly and only after prolonged exposure to low temperature. Hence, dormancy prevents precocious activation of growth. On the other hand, in the absence of dormancy and plasmodesmatal closure, growth cessation induced by short photoperiod can be quickly reversed. Thus, dormancy, unlike growth cessation, adds robustness to the mechanism that is crucial for perennial survival and longevity in the face of changing seasons.

References and Notes:

1. R. K. Singh, T. Svystun, B. AlDahmash, A. M. Jönsson, R. P. Bhalerao, Photoperiod- and temperature-mediated control of phenology in trees – a molecular perspective. *New Phytol.* **213**, 511-524 (2017).

2. C. J. Weiser, Cold resistance and injury in woody plants. *Science* **169**, 1269-1278 (1970).

3. J. E. Olsen *et al.*, Ectopic expression of oat phytochrome A in hybrid aspen changes critical daylength for growth and prevents cold acclimatization. *Plant J.* **12**, 1339-1350 (1997).

4. T. Ruttink *et al.*, A molecular timetable for apical bud formation and dormancy induction in poplar. *Plant Cell* **19**, 2370-2390 (2007).

5. A. Espinosa-Ruiz *et al.*, Differential stage-specific regulation of cyclin-dependent kinases during cambial dormancy in hybrid aspen. *Plant J.* **38**, 603-615 (2004).

6. P. L. Rinne *et al.*, Chilling of dormant buds hyperinduces FLOWERING LOCUS T and recruits GA-inducible 1,3-beta-glucanases to reopen signal conduits and release dormancy in Populus. *Plant Cell* **23**, 130-146 (2011).

7. A. Karlberg *et al.*, Analysis of global changes in gene expression during activity-dormancy cycle in hybrid aspen apex. *Plant Biotechnology* **27**, 1-16 (2010).

8. S. Penfield, J. King, Towards a systems biology approach to understanding seed dormancy and germination. *Proceedings of the Royal Society B: Biological Sciences* **276**, 3561-3569 (2009).

9. J. Leung *et al.*, Arabidopsis ABA response gene ABI1: features of a calcium-modulated protein phosphatase. *Science* **264**, 1448-1452 (1994).

10. V. A. Shepherd, P. B. Goodwin, Seasonal patterns of cell-to-cell communication in Chara corallina Klein ex Willd. I. Cell-to-cell communication in vegetative lateral branches during winter and spring. *Plant Cell Environ.* **15**, 137-150 (1992).

11. L. C. Jian, L. H. Sun, Blocking and breaking of the plasmodesmata in winter wheat seedlings in midwinter period and their role for stabilizing cold resistant ability. *Botany Research* **6**, 157-162 (1992).

12. L. Fernandez-Calvino *et al.*, Arabidopsis plasmodesmal proteome. *PLoS One* **6**, e18880 (2011).

13. S. Raffaele, E. Bayer, S. Mongrand, Upregulation of the plant protein remorin correlates with dehiscence and cell maturation: a link with the maturation of plasmodesmata? *Plant Signal Behav* **4**, 915-919 (2009).

14. C. L. Thomas, E. M. Bayer, C. Ritzenthaler, L. Fernandez-Calvino, A. J. Maule, Specific targeting of a plasmodesmal protein affecting cell-to-cell communication. *PLoS Biology* **6**, 0180-0190 (2008).

15. E. Aichinger *et al.*, CHD3 proteins and polycomb group proteins antagonistically determine cell identity in Arabidopsis. *PLoS Genet.* **5**, e1000605 (2009).

16. D. Bouyer *et al.*, Polycomb repressive complex 2 controls the embryo-to-seedling phase transition. *PLoS Genet.* **7**, e1002014 (2011).

17. C. Y. Hsu *et al.*, FLOWERING LOCUS T duplication coordinates reproductive and vegetative growth in perennial poplar. *Proc. Natl. Acad. Sci. U.S.A.* **108**, 10756-10761 (2011).

18. A. Azeez, P. Miskolczi, S. Tylewicz, R. P. Bhalerao, A Tree Ortholog of APETALA1 Mediates Photoperiodic Control of Seasonal Growth. *Curr. Biol.* **24**, 717-724 (2014).

19. M. Karimi, A. Depicker, P. Hilson, Recombinational cloning with plant gateway vectors. *Plant Physiol.* **145**, 1144-1154 (2007).

20. A. Petterle, “ABA and chromatin remodelling regulate the activity-dormancy cycle in hybrid aspen”, thesis. (Swedish University of Agricultural Sciences, Uppsala, Sweden, 2011).

21. C. Koncz, J. Schell, The promoter of TL-DNA gene 5 controls the tissue-specific expression of chimaeric genes carried by a novel type of Agrobacterium binary vector. *MGG Molecular & General Genetics* **204**, 383-396 (1986).

22. O. Nilsson *et al.*, Spatial pattern of cauliflower mosaic virus 35S promoter-luciferase expression in transgenic hybrid aspen trees monitored by enzymatic assay and non-destructive imaging. *Transgenic Research* **1**, 209-220 (1992).

23. J. Vandesompele *et al.*, Accurate normalization of real-time quantitative RT-PCR data by geometric averaging of multiple internal control genes. *Genome Biol* **3**, RESEARCH0034 (2002).

24. A. Karlberg, L. Bako, R. P. Bhalerao, Short day-mediated cessation of growth requires the downregulation of AINTEGUMENTALIKE1 transcription factor in hybrid aspen. *PLoS Genet.* **7**, (2011).

25. G. A. Tuskan *et al.*, The genome of black cottonwood, Populus trichocarpa (Torr. & Gray). *Science* **313**, 1596-1604 (2006).

26. N. Delhomme *et al.*, Guidelines for RNA-Seq data analysis. *Epigenesys Protocols (prot 67)*, (2014).

27. E. Kopylova, L. Noe, H. Touzet, SortMeRNA: fast and accurate filtering of ribosomal RNAs in metatranscriptomic data. *Bioinformatics* **28**, 3211-3217 (2012).

28. A. M. Bolger, M. Lohse, B. Usadel, Trimmomatic: a flexible trimmer for Illumina sequence data. *Bioinformatics* **30**, 2114-2120 (2014).

29. A. Dobin *et al.*, STAR: ultrafast universal RNA-seq aligner. *Bioinformatics* **29**, 15-21 (2013).

30. S. Anders, P. T. Pyl, W. Huber, HTSeq--a Python framework to work with high-throughput sequencing data. *Bioinformatics* **31**, 166-169 (2015).

31. M. I. Love, W. Huber, S. Anders, Moderated estimation of fold change and dispersion for RNA-seq data with DESeq2. *Genome Biol* **15**, 550 (2014).

32. S. Tylewicz *et al.*, Dual role of tree florigen activation complex component FD in photoperiodic growth control and adaptive response pathways. *Proc. Natl. Acad. Sci. U.S.A.* **112**, 3140-3145 (2015).

33. J. H. Venable, R. Coggeshall, A Simplified Lead Citrate Stain for Use in Electron Microscopy. *J. Cell Biol.* **25**, 407-408 (1965).

34. P. L. H. Rinne, C. Van der Schoot, Symplasmic fields in the tunica of the shoot apical meristem coordinate morphogenetic events. *Development* **125**, 1477-1485 (1998).

35. K. Nieminen *et al.*, Cytokinin signaling regulates cambial development in poplar. *Proc. Natl. Acad. Sci. U.S.A.* **105**, 20032-20037 (2008).

Acknowledgments: Funding: Grants from Vetenskapsrådet (VR-2016-04430) and Knut and Alice Wallenberg Foundation (2014-0032) to RPB are gratefully acknowledged. **Author contributions:** ST, AP, SM, PM, AA, RKS, JI performed experiments. NM and TRH performed the transcriptomics analysis. RPB, DME, JLB, YH, designed experiments and provided intellectual input. All authors contributed to writing the manuscript. **Competing interests:** The authors declare no competing interests. **Data and materials availability:** Raw RNA-seq reads are available at the European Nucleotide Archive (http://www.ebi.ac.uk/ena/) under accession number PRJEB23073. All other data needed to evaluate the conclusions in the paper are present in the paper or the Supplementary Materials.

Supplementary Materials:

Included in PDF file:

Materials and Methods
Figs. S1 to S8
Captions for table S1 in Excel file
Tables S2 to S3

Included as additional file:

Table S1

References (*19-35*)

Fig. 1. Hybrid aspen plants with attenuated ABA responses fail to establish dormancy. Buds of wild-type (A), *abi1-1* lines 1 (B) and 3 (C) after 11 weeks of short photoperiod. Unlike in WT (D), buds burst in *abi1-1* lines 1 (E) and 3 (F). TEM micrographs of apices of actively growing WT plants (G) and *abi1-1* lines 1 (H) and 3 (I) showing plasmodesmata lacking electron-dense dormancy sphincters. Sphincters are observed after 5 and 10 weeks of short photoperiod in apices of wild-type plants (J, M) (indicated with white arrows), but not *abi1-1* lines 1 (K, N) and 3 (L, O). Bar=200 nm.

Fig. 2. *PDLP1* expression restores bud dormancy in *abi1-1* plants. Buds of *abi1-1* (A) and *abi1-1/PDLP1* lines 1 (B) and 3 (C) after 11 weeks of short photoperiod. Transfer to long photoperiod results in bud burst in *abi1-1* plants (D), but not in *abi1-1/PDLP1* lines 1 (E) and 3 (F).

Fig. 3. *PKL* downregulation restores dormancy sphincters and bud dormancy in *abi1-1* plants. TEM micrographs of apices of actively growing *abi1-1* plants (A) and *abi1-1/PKL*RNAi lines 9 (B) and 11 (C) showing plasmodesmata lacking electron-dense dormancy sphincters. After 5 and 10 weeks of short photoperiod, sphincters were not observed in *abi1-1* apices (D, G), but were present in *abi1-1/PKL*RNAi apices of lines 9 (E, H) and 11 (F, I) (arrows). Bar=500 nm. Buds of *abi1-1* plants (J) and *abi1-1/PKL*RNAi lines 9 (K) and 11 (L) after 11 weeks of

short photoperiod. Following shift to long photoperiod, buds burst in *abi1-1* plants (M), but not in *abi1-1/PKL*RNAi lines 9 (N) and 11 (O).

Fig. 4. *FT1*-expressing stocks can reactivate growth in *abi1-1* scions under short photoperiod. Wild-type (WT) and *abi1-1* buds after 10 weeks of short photoperiod before grafting, and a further 2 and 7 weeks of short photoperiod following grafting of WT and *abi1-1* scions on *FT1*-expressing stocks. Buds remained dormant in WT scions, but burst in *abi1-1* scions.

Supplementary Materials for

Photoperiodic Control of Seasonal Growth is Mediated by ABA Acting on Cell-Cell Communication

S. Tylewicz, A. Petterle, S. Marttila, P. Miskolczi, A. Azeez, R. K. Singh, J. Immanen, N. Mähler, T. R. Hvidsten, D. M. Eklund, J. L. Bowman, Y. Helariutta, R. P. Bhalerao

Correspondence to: rishi.bhalerao@slu.se

Supplement:

Included in PDF file:

- Materials and Methods
- Figs. S1 to S8
- Captions for table S1 in Excel file
- Tables S2 to S3

Included as additional file:

- Table S1

References (*19-35*)

Materials and Methods

Plant material and growth conditions

Hybrid aspen (*Populus tremula x tremuloides*) clone T89 (wild type) and the transgenic plants were cultivated in half-strength MS medium (Duchefa) under sterile conditions for 5 weeks and then transferred to soil and grown for another 4 weeks in the greenhouse (16 hour light/8 hour dark cycles, 22°C and 66% relative humidity) prior to analysis of bud dormancy. For dormancy assessment, plants were shifted from the greenhouse to controlled growth chambers and grown under long photoperiod (16 hour, 20°C light/8 hour, 15°C cycles) for 1 week for acclimatization followed by exposure to 11 weeks of short photoperiod (8 hour, 20°C light/16 hour, 15°C dark cycles). Metal halide bulbs (HQI-T 400W daylight) were used as light source producing approximately 220 µmol m-2 s-1 radiation. Following short photoperiod treatment, plants were shifted back to long photoperiod conditions and bud burst was monitored for at least 3 months to assess the establishment of bud dormancy (5). Shoot apices were collected for gene expression analyses after 0, 6 and 10 weeks of short photoperiod, at the same time of day (14:00 hours) and stored at −80 °C until further use. For analysis of ABA responsive gene expression, apices (after removal of any leaves separated from the apex) were cut and placed in MS medium with or without 50 micromolar ABA in MS medium for 4 hours with gentle shaking followed by rinsing with fresh MS and freezing until isolation of RNA. Three pools of three apices from three independent plants were collected for every sample providing three biological replicates. Photographs of apices were taken using a Canon EOS digital camera to monitor bud formation.

Generation of plasmids

To generate the PDLP1-GFP construct, a fragment containing PDLP1-GFP was amplified from plasmid (a kind gift from Prof. Maule, John Innes Institute, UK) using PDLP-For 5'-CACCGGATCCATGAAACTCACCTATCAAT-3' and EGFP-BamRev 5'-TTTTTGGATCCCTACTTGTACAGCTCGT-3' primers. This fragment was cloned into pENTR/D-TOPO (Invitrogen) and subsequently transferred into the pH2GW7 plant transformation vector to generate a plasmid designated pH2GW7-PDLP1-GFP. To generate the PKLRNAi construct, a 346 bp fragment was amplified from hybrid aspen cDNA using 5'-CACCCAGATGATATTATACTGCGCTACCC-3' and 5'-TAACAGTGCTGGGTTTGCAG-3' primers. This fragment was then cloned into pENTR/D-TOPO and subsequently transferred into pK7GWIWG2 (I) (*19*).

Plant transformation

The generation of hybrid aspen plants expressing *abi1-1* has been previously described (*20*). The transformation constructs were introduced into *Agrobacterium* strain GV3101pmp90RK (*21*), then used to transform hybrid aspen clone T89 as previously described (*22*). The vector pH2GW7-PDLP1-GFP was used to transform *abi1-1* plants to generate *PDLP1-GFP*-overexpression in the *abi1-1* background. The vector pK7GWIWG2 (I)-PKLRNAi was used to transform *abi1-1* plants to generate *PKL*RNAi overexpression in the *abi1-1* background.

RNA isolation and quantitative real-time PCR (qRT-PCR) analysis

Total RNA was extracted, using an Aurum Total RNA kit (Bio-Rad) or RNeasy® Plus Universal Kit (Qiagen), from tissue samples taken at the same time of day. Portions (10 µg) of total RNA were treated with RNase-Free DNase (Qiagen) and cleaned using an RNeasy® Mini Kit (Qiagen). One µg of the RNA from each sample was used to generate cDNA using an iScript cDNA synthesis kit (BioRad). Selected (*UBQ*/*TIP41*-like) reference genes were validated using GeNorm Software (*23*). qRT-PCR analyses were carried out with a Roche LightCycler 480 II instrument and relative expression values were calculated using the Δ-ct-method, as previously described (*24*).

RNA sequencing and analysis

RNAseq was performed at BGI (Beijing, China) using RNA isolated from apices of wild type and *abi1-1*/line 1 at 0, 6 and 10 weeks long photoperiod. RNA-Seq reads were mapped to version 3 of the Populus trichocarpa genome (*25*) using the approach described earlier (*26*). In short, ribosomal RNA was filtered using sortmerna (*27*) and consequently trimmed using trimmomatic (*28*) before being mapped to the genome using STAR (*29*). Reads per gene were counted using htseq-count from HTSeq (*30*) and differential expression analysis was performed on raw counts using DESeq2 (*31*). Genes with a Benjamini-Hochberg adjusted p-value < 0.05 and an absolute $\log_2$ fold change > 1 were considered differentially expressed. For further analysis of poplar homologs of Arabidopsis plasmodesmata enriched genes, an adjusted p-value < 0.05 and an absolute log2 fold change >0.2 were used as filtering criteria. Raw RNA-seq reads are available at the European Nucleotide Archive (http://www.ebi.ac.uk/ena/) under accession number PRJEB23073.

Western blot analysis

Total protein was extracted from leaves of untransformed control and two independent PDLP1-GFP transformants. Western blotting was performed as described earlier (*32*). PDLP1-GFP levels were analyzed using anti-GFP antibodies (Novus Biologicals).

Transmission electron microscopy

Hybrid aspen buds and actively growing apices collected after 0, 5 and 10 weeks of short photoperiod were fixed in 2% glutaraldehyde and 2% paraformaldehyde in 0.02 M cacodylate buffer (pH 7.2), combined with 1% tannic acid; postfixed 1% OsO_4 in water, dehydrated, infiltrated and embedded in Spurr's resin (Ted Pella). Ultra-thin sections were stained with uranyl acetate and lead citrate (*33*), and examined in transmission electron microscope (JEOL). For quantitative analysis, dormancy sphincters, visualized as electron-dense dots and marking closed plasmodesmata, were counted as percentage of the total number of counted plasmodesmata (*34*). In each experiment in which dormancy sphincters were examined, these were counted in samples from three independent plants representing each genotype and timepoint combination. Results are reported as percentage plasmodesmata with closed plasmodesmata.

Grafting experiments

Soil-grown wild type and *abi1-1* plants were exposed to short photoperiod conditions for 10 weeks as already described. Apices of wild type and *abi1-1* plants were grafted onto *FT1*-overexpressing plants, as previously reported (*35*), then the grafted plants were returned to the short photoperiod chamber and monitored for bud break.

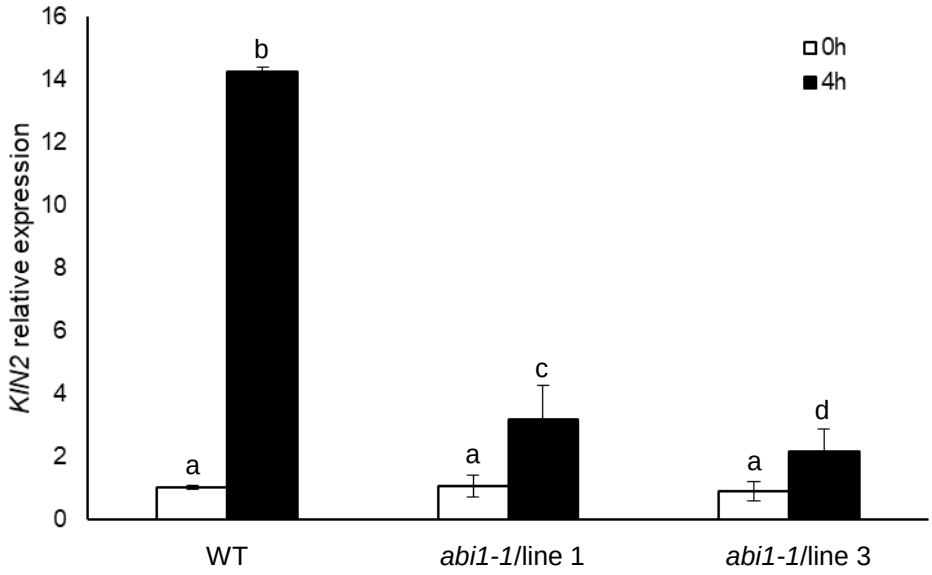

Fig. S1

Expression of *abi1-1* in hybrid aspen leads to attenuation of ABA responses. Relative transcript levels of *KIN2* before and after ABA treatment of wild type (WT) and *abi1-1* plants (line 1 and line 3). Bars show the average of three biological replicates ± standard error (SE). Letters (a–d) over the bars indicate significant differences at $P<0.05$ (means followed by the same letter are not significantly different at $P<0.05$).

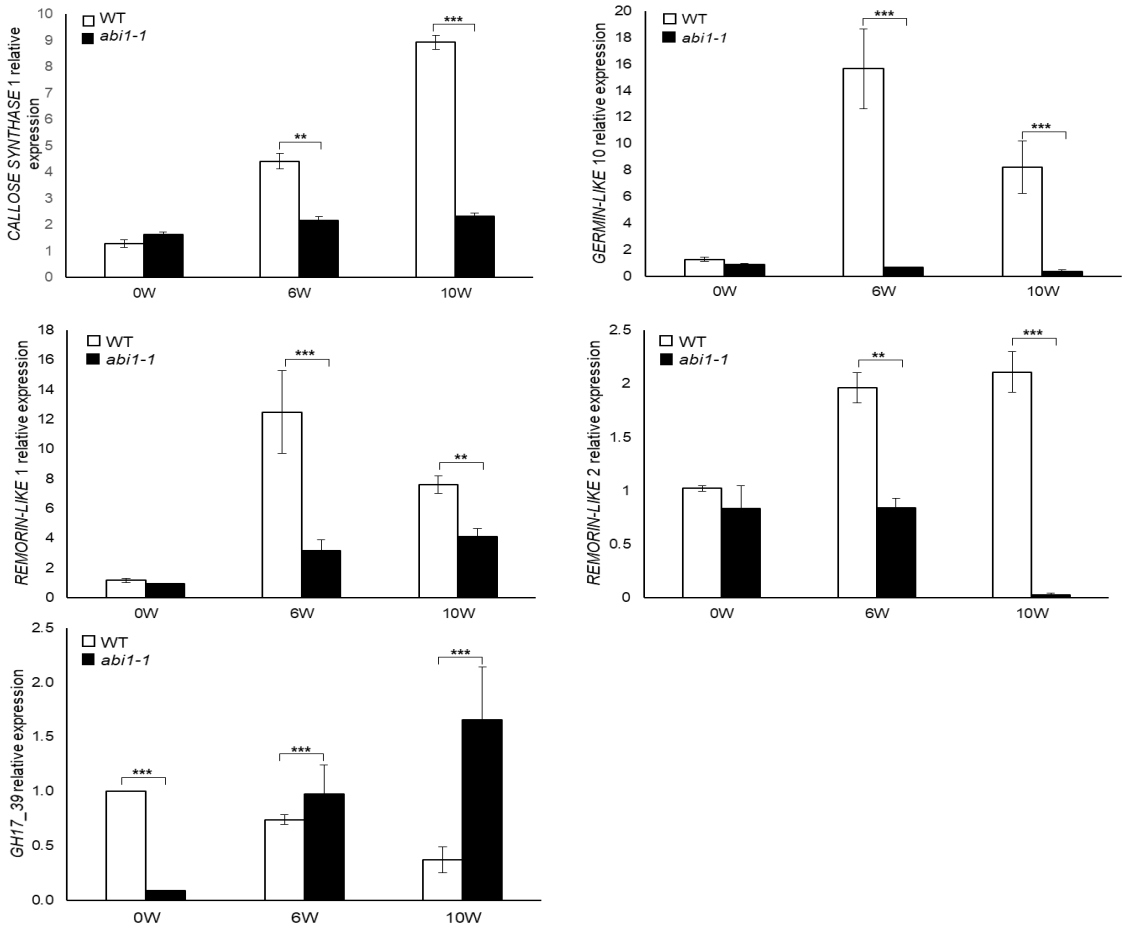

Fig. S2

Relative expression of plasmodesmata-associated marker genes in apices of wild-type and *abi1-1* (line 1) plants before (0W) and after 6 and 10 weeks (6W and 10W) of short photoperiod treatment. Bars show the average of three biological replicates ± SE. Asterisks (**) indicate very significant differences at P<0.01 and *** extremely significant (P<0.001) with respect to WT at each time point.

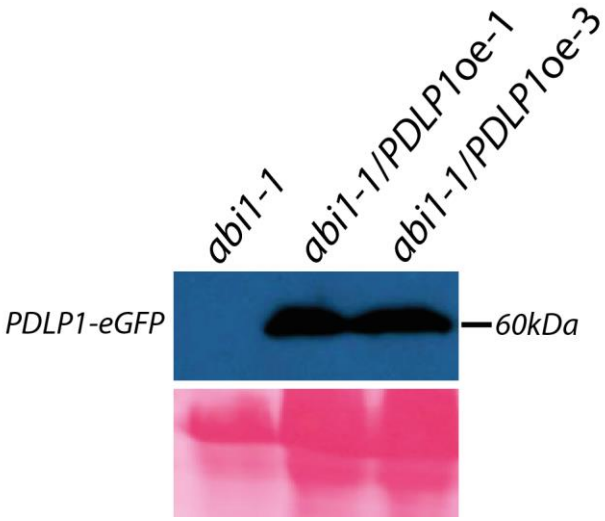

Fig. S3

Western blot analysis of PDLP1-eGFP levels in *abi1-1* apices (controls) and two independent PDLP1-eGFP transformed *abi1-1* lines (upper panel). The lower panel shows the same blot stained with Ponceau S.

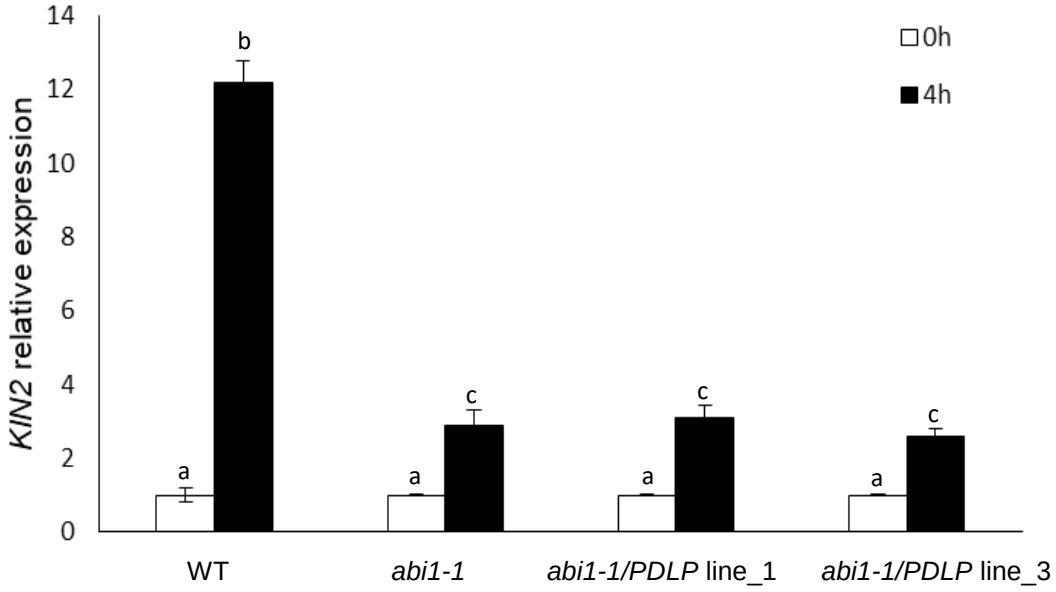

Fig. S4

Expression of PDLP in *abi1-1* does not leads to attenuation of ABA responses. Relative transcript levels of *KIN2* before and after ABA treatment of wild type (WT), *abi1-1* plants and *abi1-1* plants expressing PDLP (*abi1-1*/*PDLP* lines 1 and line 3). Bars show the average of three biological replicates ± SE. Letters (a–c) over the bars indicate significant differences at $P<0.05$ (means followed by the same letter are not significantly different at $P<0.05$).

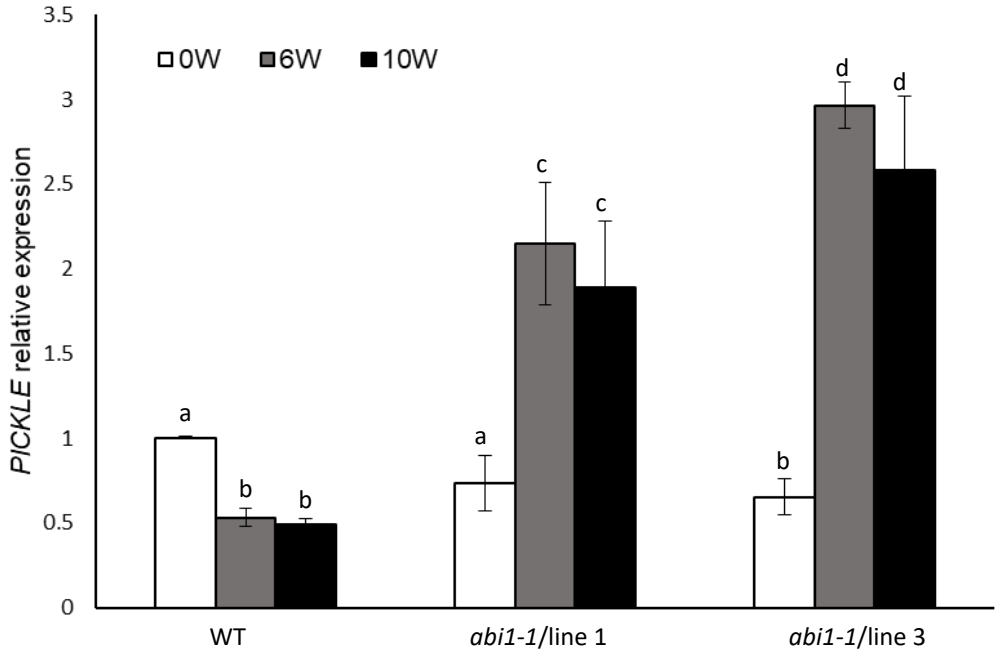

Fig. S5

Altered *PKL* expression in *abi1-1* plants after short photoperiod. *PKL* transcript levels are reduced in WT but increased in *abi1-1* plants after short photoperiod. The graph shows relative levels of *PKL* in WT and *abi1-1* plants before (0W) and after 6 and 10 weeks (6W and 10W) of short photoperiod treatment. Bars show the average of three biological replicates ± SE. Letters (a–d) over the bars indicate significant differences at $P<0.05$ (means followed by the same letter are not significantly different at $P<0.05$).

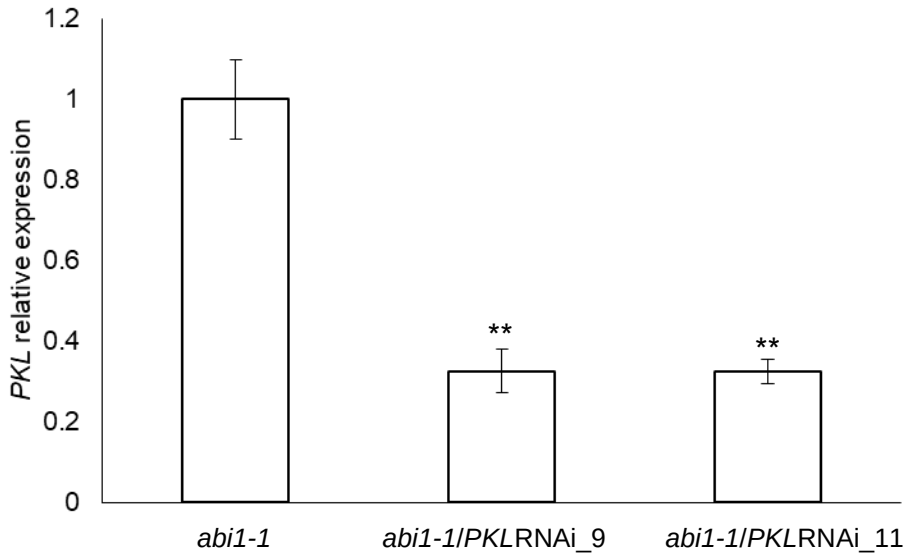

Fig. S6

***PKL* transcript levels are reduced in *abi1-1*/*PKL*RNAi plants.** The graph shows relative levels of *PKL* in *abi1-1* and *abi1-1*/*PKL*RNAi lines. Bars show the average of three biological replicates ± SE. Asterisk (**) indicate a significant difference at P<0.01 with respect to control (*abi1-1*) plants.

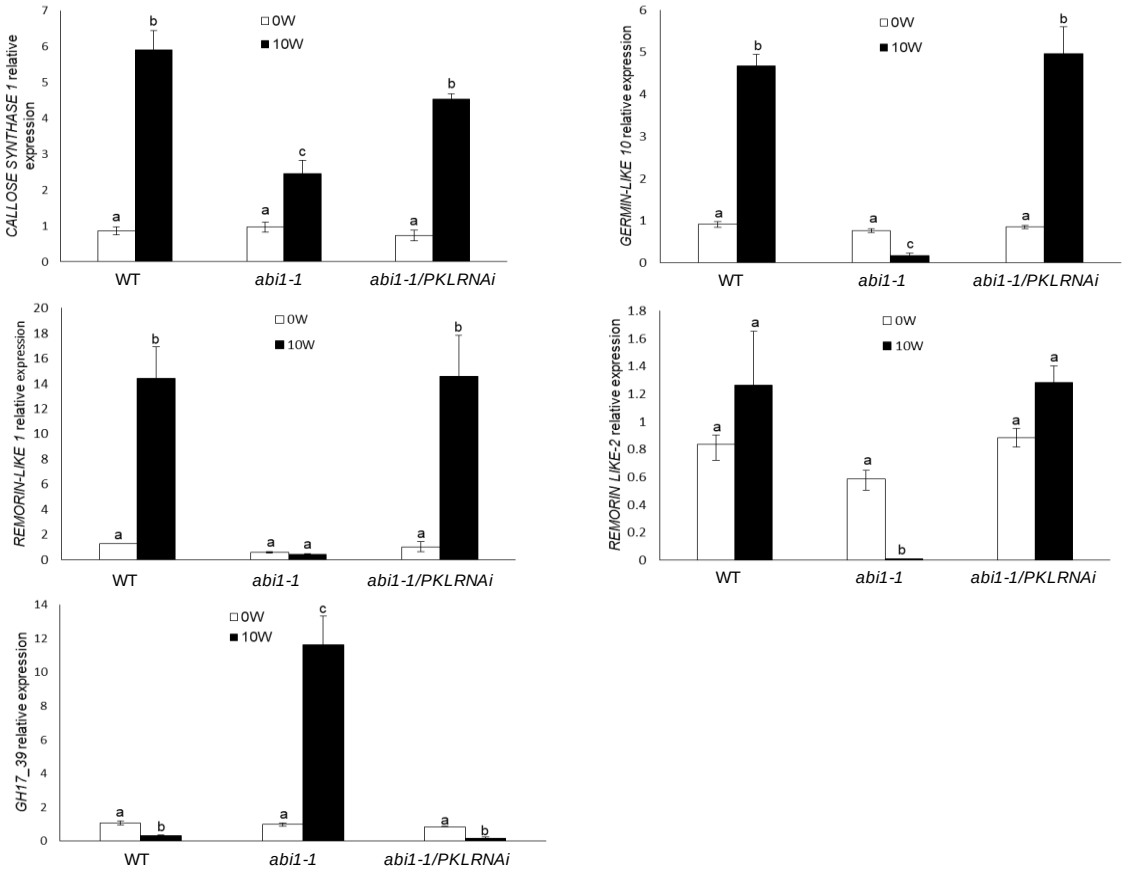

Fig. S7

Relative expression levels of plasmodesmata-associated marker genes in apices of wild-type, *abi1-1* (line 1) and *abi1-1*/*PKL*RNAi plants before (0W) and after 10 week (10W) of short photoperiod treatment. Bars show the average of three biological replicates ± SE. Letters (a–c) over the bars indicate significant differences at $P<0.05$ (means followed by the same letter are not significantly different at $P<0.05$).

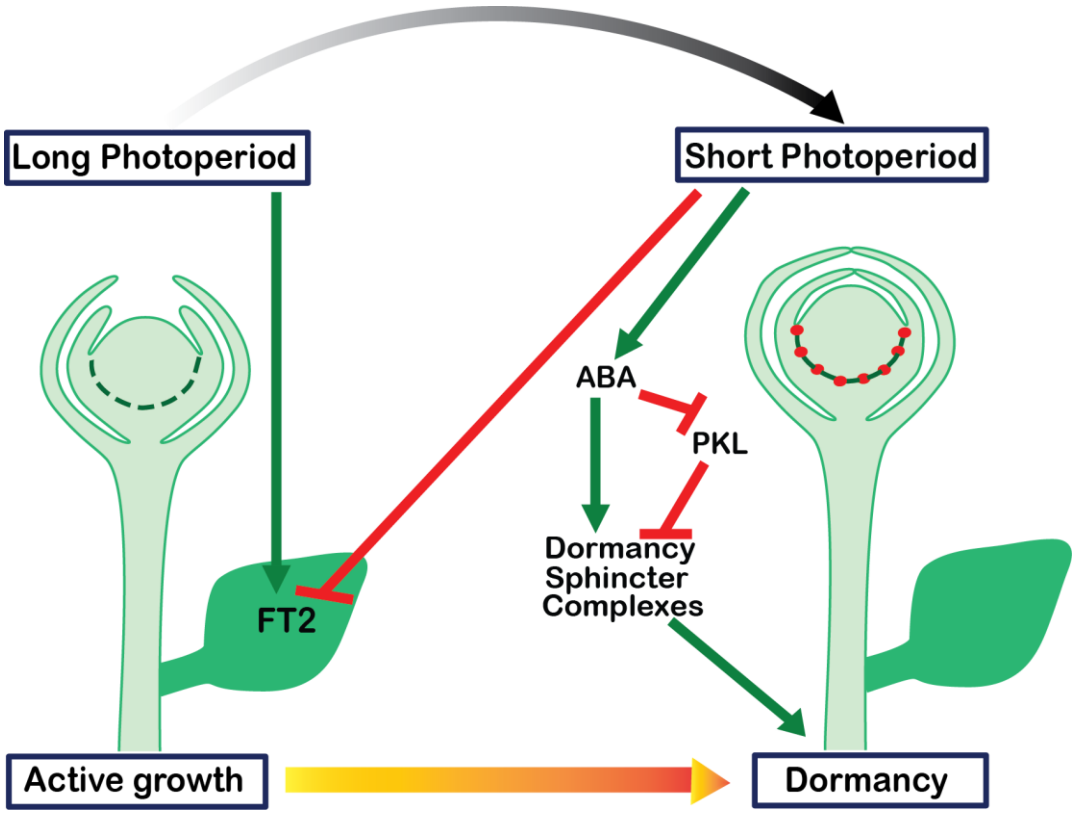

Fig. S8

Schematic model of photoperiodic control of bud dormancy. In long photoperiod, plasmodesmata are open, allowing SAM access to growth-promotive signals, e.g. FT, permitting growth. Short photoperiod suppress *FT* expression and downregulate *PKL*, inducing ABA-mediated formation of dormancy sphincters, limiting access of SAM and promoting dormancy.

Table S1 caption:

Differential expression results. Each sheet contains results for one comparison e.g. WT_6w_vs_0w contains comparisons of gene expression between 6 weeks and 0 weeks of short photoperiod treatment in the wild-type. Columns A-C contain gene information from Phytozome (https://phytozome.jgi.doe.gov). Column D (baseMean): mean expression over e.g. all 6 weeks and 0 weeks replicates. Column E (log2FoldChange): log2 fold change expression between e.g. 6 weeks and 0 weeks of short photoperiod treatment. Column F (lfcSE): standard error of the log2 fold change. Column G (pvalue): p-value for the comparison. Column H (padj): Benjamini-Hochberg adjusted p-value.

Table S2

List of *Populus trichocarpa* genes that are homologous to the genes that were identified in the plasmodesmata fraction of *Arabidopsis thaliana*, based on best BLAST hits. Columns contain gene information from PopGenIE and AtGenIE (http://popgenie.org/, http://atgenie.org/).

P. trichocarpa gene ID	At gene ID	Description in Atgenie	At synonyms
Potri.001G065900	AT1G28110	serine carboxypeptidase-like 45	SCPL45
Potri.001G092200	AT1G64390	glycosyl hydrolase 9C2	AtGH9C2,GH9C2
Potri.001G108700	AT1G63120	RHOMBOID-like 2	ATRBL2,RBL2
Potri.001G112100	AT2G42010	phospholipase D beta 1	PLDBETA,PLDBETA1
Potri.001G129300	AT4G28050	tetraspanin7	TET7
Potri.001G141400	AT5G46700	Tetraspanin family protein	TET1,TRN2
Potri.001G200400	AT3G13750	beta galactosidase 1	BGAL1
Potri.001G236400	AT3G46010	actin depolymerizing factor 1	ADF1,atadf,ATADF1
Potri.001G240900	AT2G39700	expansin A4	ATEXP4,ATEXPA4,ATHEXP ALPHA 1.6,EXPA4
Potri.001G278300	AT5G58600	Plant protein of unknown function (DUF828)	PMR5,TBL44
Potri.001G283000	AT1G74520	HVA22 homologue A	ATHVA22A,HVA22A
Potri.001G311700	AT5G64260	EXORDIUM like 2	EXL2
Potri.001G342200	AT5G14420	RING domain ligase2	RGLG2
Potri.001G357800	AT1G30460	cleavage and polyadenylation specificity factor 30	ATCPSF30,CPSF30
Potri.001G423700	AT3G20500	purple acid phosphatase 18	ATPAP18,PAP18
Potri.001G442400	AT4G20380	LSD1 zinc finger family protein	LSD1
Potri.002G029300	AT2G16430	purple acid phosphatase 10	ATPAP10,PAP10
Potri.002G060400	AT4G14130	xyloglucan endotransglucosylase/hydrolase 15	XTH15,XTR7
Potri.002G060500	AT4G14130	xyloglucan endotransglucosylase/hydrolase 15	XTH15,XTR7
Potri.002G098900	AT5G64260	EXORDIUM like 2	EXL2
Potri.002G120600	AT4G24220	NAD(P)-binding Rossmann-fold superfamily protein	AWI31,VEP1
Potri.002G120700	AT4G24220	NAD(P)-binding Rossmann-fold superfamily protein	AWI31,VEP1
Potri.002G129400	AT2G26510	Xanthine/uracil permease family protein	PDE135
Potri.002G145400	AT3G60720	plasmodesmata-located protein 8	PDLP8
Potri.002G152100	AT2G42010	phospholipase D beta 1	PLDBETA,PLDBETA1
Potri.002G200300	AT1G02730	cellulose synthase-like D5	ATCSLD5,CSLD5,SOS6
Potri.002G257300	AT1G04520	plasmodesmata-located protein 2	PDLP2
Potri.003G038500	AT3G13750	beta galactosidase 1	BGAL1
Potri.003G093000	AT5G46700	Tetraspanin family protein	TET1,TRN2
Potri.003G122900	AT1G63120	RHOMBOID-like 2	ATRBL2,RBL2
Potri.003G134500	AT4G24220	NAD(P)-binding Rossmann-fold superfamily protein	AWI31,VEP1
Potri.003G139600	AT1G64390	glycosyl hydrolase 9C2	AtGH9C2,GH9C2
Potri.003G164000	AT1G28110	serine carboxypeptidase-like 45	SCPL45
Potri.004G010100	AT4G22010	SKU5 similar 4	sks4
Potri.004G042400	AT4G25810	xyloglucan endotransglycosylase 6	XTH23,XTR6
Potri.004G100700	AT3G02540	Rad23 UV excision repair protein family	RAD23-3,RAD23C
Potri.004G123200	AT1G69530	expansin A1	AT-EXP1,ATEXP1,ATEXPA1,ATHEXP ALPHA 1.2,EXP1,EXPA1
Potri.004G160100	AT2G16430	purple acid phosphatase 10	ATPAP10,PAP10
Potri.004G160200	AT2G16430	purple acid phosphatase 10	ATPAP10,PAP10
Potri.004G173900	AT4G34980	subtilisin-like serine protease 2	SLP2
Potri.004G184500	AT2G27600	AAA-type ATPase family protein	ATSKD1,SKD1,VPS4
Potri.004G206600	AT2G17230	EXORDIUM like 5	EXL5
Potri.005G000100	AT5G26742	DEAD box RNA helicase (RH3)	emb1138
Potri.005G000200	AT5G26742	DEAD box RNA helicase (RH3)	emb1138
Potri.005G000500	AT5G26742	DEAD box RNA helicase (RH3)	emb1138
Potri.005G007200	AT4G25810	xyloglucan endotransglycosylase 6	XTH23,XTR6
Potri.005G128800	AT4G36860	LIM domain-containing protein	DAR1
Potri.005G128900	AT4G36860	LIM domain-containing protein	DAR1
Potri.005G152100	AT1G69700	HVA22 homologue C	ATHVA22C,HVA22C

Potri.005G163000	AT5G64260	EXORDIUM like 2	EXL2
Potri.005G201200	AT4G14130	xyloglucan endotransglucosylase/hydrolase 15	XTH15,XTR7
Potri.005G233400	AT2G27190	purple acid phosphatase 12	ATPAP1,ATPAP12,PAP1,PAP12
Potri.006G002600	AT5G14420	RING domain ligase2	RGLG2
Potri.006G003600	AT1G60870	maternal effect embryo arrest 9	MEE9
Potri.006G006100	AT5G63530	farnesylated protein 3	ATFP3,FP3
Potri.006G032100	AT2G40830	RING-H2 finger C1A	RHC1A
Potri.006G034200	AT3G56640	exocyst complex component sec15A	SEC15A
Potri.006G036000	AT1G28110	serine carboxypeptidase-like 45	SCPL45
Potri.006G036400	AT2G33530	serine carboxypeptidase-like 46	scpl46
Potri.006G036500	AT1G28110	serine carboxypeptidase-like 45	SCPL45
Potri.006G058500	AT5G06860	polygalacturonase inhibiting protein 1	ATPGIP1,PGIP1
Potri.006G058600	AT5G06860	polygalacturonase inhibiting protein 1	ATPGIP1,PGIP1
Potri.006G071200	AT4G25810	xyloglucan endotransglycosylase 6	XTH23,XTR6
Potri.006G098700	AT1G74720	C2 calcium/lipid-binding plant phosphoribosyltransferase family protein	QKY
Potri.006G144500	AT3G13750	beta galactosidase 1	BGAL1
Potri.006G150400	AT2G19580	tetraspanin2	TET2
Potri.006G169900	AT4G25810	xyloglucan endotransglycosylase 6	XTH23,XTR6
Potri.006G170000	AT4G25810	xyloglucan endotransglycosylase 6	XTH23,XTR6
Potri.006G170100	AT4G25810	xyloglucan endotransglycosylase 6	XTH23,XTR6
Potri.006G177900	AT2G23810	tetraspanin8	TET8
Potri.006G204200	AT3G11660	NDR1/HIN1-like 1	NHL1
Potri.007G032500	AT4G36860	LIM domain-containing protein	DAR1
Potri.007G083400	AT3G45970	expansin-like A1	ATEXLA1,ATEXPL1,ATHEXP BETA 2.1,EXLA1,EXPL1
Potri.008G010900	AT5G04990	SAD1/UNC-84 domain protein 1	ATSUN1,SUN1
Potri.008G018300	AT5G04850	SNF7 family protein	VPS60.2
Potri.008G022300	AT2G27600	AAA-type ATPase family protein	ATSKD1,SKD1,VPS4
Potri.008G032100	AT5G48450	SKU5 similar 3	sks3
Potri.008G038100	AT5G03300	adenosine kinase 2	ADK2
Potri.008G057100	AT2G39700	expansin A4	ATEXP4,ATEXPA4,ATHEXP ALPHA 1.6,EXPA4
Potri.008G088300	AT1G69530	expansin A1	AT-EXP1,ATEXP1,ATEXPA1,ATHEXP ALPHA 1.2,EXP1,EXPA1
Potri.008G095300	AT1G18650	plasmodesmata callose-binding protein 3	PDCB3
Potri.008G119700	AT3G02540	Rad23 UV excision repair protein family	RAD23-3,RAD23C
Potri.008G133500	AT2G01660	plasmodesmata-located protein 6	PDLP6
Potri.008G171700	AT1G04520	plasmodesmata-located protein 2	PDLP2
Potri.008G183600	AT5G14420	RING domain ligase2	RGLG2
Potri.008G193700	AT1G10510	RNI-like superfamily protein	emb2004
Potri.009G015100	AT3G45600	tetraspanin3	TET3
Potri.009G031800	AT2G39700	expansin A4	ATEXP4,ATEXPA4,ATHEXP ALPHA 1.6,EXPA4
Potri.009G072800	AT5G58600	Plant protein of unknown function (DUF828)	PMR5,TBL44
Potri.009G078500	AT1G74520	HVA22 homologue A	ATHVA22A,HVA22A
Potri.009G092000	AT4G24220	NAD(P)-binding Rossmann-fold superfamily protein	AWI31,VEP1
Potri.009G100500	AT4G34980	subtilisin-like serine protease 2	SLP2
Potri.009G121200	AT2G16430	purple acid phosphatase 10	ATPAP10,PAP10
Potri.009G133400	AT4G34980	subtilisin-like serine protease 2	SLP2
Potri.009G144200	AT2G27600	AAA-type ATPase family protein	ATSKD1,SKD1,VPS4
Potri.009G144300	AT2G27600	AAA-type ATPase family protein	ATSKD1,SKD1,VPS4
Potri.009G167800	AT2G17230	EXORDIUM like 5	EXL5
Potri.010G049600	AT5G14420	RING domain ligase2	RGLG2
Potri.010G065800	AT1G04520	plasmodesmata-located protein 2	PDLP2
Potri.010G108100	AT2G01660	plasmodesmata-located protein 6	PDLP6
Potri.010G114200	AT1G71040	Cupredoxin superfamily protein	LPR2
Potri.010G126200	AT3G02540	Rad23 UV excision repair protein family	RAD23-3,RAD23C
Potri.010G158900	AT1G18650	plasmodesmata callose-binding protein 3	PDCB3
Potri.010G167200	AT1G69530	expansin A1	AT-EXP1,ATEXP1,ATEXPA1,ATHEXP ALPHA 1.2,EXP1,EXPA1
Potri.010G202500	AT2G39700	expansin A4	ATEXP4,ATEXPA4,ATHEXP ALPHA 1.6,EXPA4

Potri.010G224300	AT5G03300	adenosine kinase 2	ADK2
Potri.010G237100	AT2G27600	AAA-type ATPase family protein	ATSKD1,SKD1,VPS4
Potri.010G247900	AT5G04990	SAD1/UNC-84 domain protein 1	ATSUN1,SUN1
Potri.011G052400	AT4G04970	glucan synthase-like 1	ATGSL01,ATGSL1,GSL01,GSL1
Potri.011G077200	AT4G18040	eukaryotic translation initiation factor 4E	AT.EIF4E1,CUM1,EIF4E,eIF4E1
Potri.011G077400	AT4G14130	xyloglucan endotransglucosylase/hydrolase 15	XTH15,XTR7
Potri.011G089800	AT1G30460	cleavage and polyadenylation specificity factor 30	ATCPSF30,CPSF30
Potri.011G089900	AT1G30460	cleavage and polyadenylation specificity factor 30	ATCPSF30,CPSF30
Potri.011G135500	AT4G27080	PDI-like 5-4	ATPDI7,ATPDIL5-4,PDI7,PDIL5-4
Potri.011G138200	AT3G20500	purple acid phosphatase 18	ATPAP18,PAP18
Potri.011G154800	AT4G20380	LSD1 zinc finger family protein	LSD1
Potri.012G006100	AT5G24520	Transducin/WD40 repeat-like superfamily protein	ATTTG1,TTG,TTG1,URM23
Potri.012G061600	AT5G61030	glycine-rich RNA-binding protein 3	GR-RBP3
Potri.012G065700	AT1G18650	plasmodesmata callose-binding protein 3	PDCB3
Potri.012G069300	AT1G74520	HVA22 homologue A	ATHVA22A,HVA22A
Potri.012G090100	AT5G14420	RING domain ligase2	RGLG2
Potri.012G101400	AT5G63530	farnesylated protein 3	ATFP3,FP3
Potri.012G105500	AT1G28110	serine carboxypeptidase-like 45	SCPL45
Potri.012G128100	AT5G51550	EXORDIUM like 3	EXL3
Potri.013G005700	AT4G25810	xyloglucan endotransglycosylase 6	XTH23,XTR6
Potri.013G048200	AT1G04520	plasmodesmata-located protein 2	PDLP2
Potri.013G118500	AT2G42570	TRICHOME BIREFRINGENCE-LIKE 39	TBL39
Potri.013G152400	AT4G03210	xyloglucan endotransglucosylase/hydrolase 9	XTH9
Potri.014G019300	AT4G24220	NAD(P)-binding Rossmann-fold superfamily protein	AWI31,VEP1
Potri.014G019400	AT4G24220	NAD(P)-binding Rossmann-fold superfamily protein	AWI31,VEP1
Potri.014G019500	AT4G24220	NAD(P)-binding Rossmann-fold superfamily protein	AWI31,VEP1
Potri.014G019600	AT4G24220	NAD(P)-binding Rossmann-fold superfamily protein	AWI31,VEP1
Potri.014G019700	AT4G24220	NAD(P)-binding Rossmann-fold superfamily protein	AWI31,VEP1
Potri.014G035800	AT2G26510	Xanthine/uracil permease family protein	PDE135
Potri.014G067000	AT3G60720	plasmodesmata-located protein 8	PDLP8
Potri.014G074700	AT2G42010	phospholipase D beta 1	PLDBETA,PLDBETA1
Potri.014G125100	AT1G02730	cellulose synthase-like D5	ATCSLD5,CSLD5,SOS6
Potri.014G126000	AT5G64260	EXORDIUM like 2	EXL2
Potri.014G148600	AT1G74520	HVA22 homologue A	ATHVA22A,HVA22A
Potri.014G154500	AT4G22010	SKU5 similar 4	sks4
Potri.014G177700	AT5G48450	SKU5 similar 3	sks3
Potri.015G002600	AT5G24520	Transducin/WD40 repeat-like superfamily protein	ATTTG1,TTG,TTG1,URM23
Potri.015G055700	AT2G23810	tetraspanin8	TET8
Potri.015G057400	AT5G61030	glycine-rich RNA-binding protein 3	GR-RBP3
Potri.015G057800	AT1G18650	plasmodesmata callose-binding protein 3	PDCB3
Potri.015G062800	AT1G74520	HVA22 homologue A	ATHVA22A,HVA22A
Potri.015G086200	AT5G14420	RING domain ligase2	RGLG2
Potri.015G104700	AT1G28110	serine carboxypeptidase-like 45	SCPL45
Potri.015G129700	AT5G51550	EXORDIUM like 3	EXL3
Potri.016G003000	AT5G14420	RING domain ligase2	RGLG2
Potri.016G004300	AT1G60870	maternal effect embryo arrest 9	MEE9
Potri.016G029300	AT2G40830	RING-H2 finger C1A	RHC1A
Potri.016G032100	AT3G56640	exocyst complex component sec15A	SEC15A
Potri.016G034300	AT1G28110	serine carboxypeptidase-like 45	SCPL45
Potri.016G034400	AT1G28110	serine carboxypeptidase-like 45	SCPL45
Potri.016G034500	AT1G28110	serine carboxypeptidase-like 45	SCPL45
Potri.016G034600	AT2G33530	serine carboxypeptidase-like 46	scpl46
Potri.016G034700	AT1G28110	serine carboxypeptidase-like 45	SCPL45
Potri.016G034900	AT1G28110	serine carboxypeptidase-like 45	SCPL45
Potri.016G046100	AT2G33330	plasmodesmata-located protein 3	PDLP3
Potri.016G049400	AT5G06860	polygalacturonase inhibiting protein 1	ATPGIP1,PGIP1
Potri.016G049600	AT5G06860	polygalacturonase inhibiting protein 1	ATPGIP1,PGIP1
Potri.016G071500	AT3G11660	NDR1/HIN1-like 1	NHL1
Potri.016G097500	AT2G39700	expansin A4	ATEXP4,ATEXPA4,ATHEXP ALPHA 1.6,EXPA4
Potri.016G113800	AT1G74720	C2 calcium/lipid-binding plant phosphoribosyltransferase family protein	QKY
Potri.017G030300	AT4G24220	NAD(P)-binding Rossmann-fold superfamily protein	AWI31,VEP1

Potri.017G030400	AT4G24220	NAD(P)-binding Rossmann-fold superfamily protein	AWI31,VEP1
Potri.017G030600	AT4G24220	NAD(P)-binding Rossmann-fold superfamily protein	AWI31,VEP1
Potri.017G030700	AT4G24220	NAD(P)-binding Rossmann-fold superfamily protein	AWI31,VEP1
Potri.017G051700	AT5G64260	EXORDIUM like 2	EXL2
Potri.017G102800	AT2G40830	RING-H2 finger C1A	RHC1A
Potri.017G114000	AT3G02540	Rad23 UV excision repair protein family	RAD23-3,RAD23C
Potri.017G139000	AT1G74520	HVA22 homologue A	ATHVA22A,HVA22A
Potri.018G094900	AT4G25810	xyloglucan endotransglycosylase 6	XTH23,XTR6
Potri.018G095100	AT4G25810	xyloglucan endotransglycosylase 6	XTH23,XTR6
Potri.018G095200	AT4G25810	xyloglucan endotransglycosylase 6	XTH23,XTR6
Potri.018G099800	AT2G23810	tetraspanin8	TET8
Potri.019G045200	AT3G45600	tetraspanin3	TET3
Potri.019G069300	AT1G71380	cellulase 3	ATCEL3,ATGH9B3,CEL3
Potri.019G090200	AT2G42570	TRICHOME BIREFRINGENCE-LIKE 39	TBL39
Potri.019G125000	AT4G03210	xyloglucan endotransglucosylase/hydrolase 9	XTH9
Potri.T112400	AT4G14130	xyloglucan endotransglucosylase/hydrolase 15	XTH15,XTR7
Potri.T121300	AT2G17230	EXORDIUM like 5	EXL5
Potri.T121400	AT2G17230	EXORDIUM like 5	EXL5
Potri.T162000	AT5G61030	glycine-rich RNA-binding protein 3	GR-RBP3
Potri.T180000	AT2G42010	phospholipase D beta 1	PLDBETA,PLDBETA1
Potri.T180200	AT4G14130	xyloglucan endotransglucosylase/hydrolase 15	XTH15,XTR7

Table S3

Sequences of primers used in quantitative RT-PCR

REMORIN-LIKE 1 forward	GCAGATCCAACTGCTGATGA
REMORIN-LIKE 1 reverse	CTCATTTTCCACCCATGCTT
REMORIN-LIKE 2 forward	CGAACAGCTTTAGGCAAACC
REMORIN-LIKE 2 reverse	TCCTGTCGTCTGCATTTGAG
CALLOSE SYNTHASE 1 forward	TAAATAACCGTGGAGGGATTGG
CALLOSE SYNTHASE 1 reverse	GAGCCGAACAAGAGTTGGAAGT
GERMIN-LIKE 10 forward	TTACATGCAAGGCAGAGACG
GERMIN-LIKE 10 reverse	AGGCCTGGGATTTTCTCAAC
PICKLE-LIKE forward	TGGACTGTGAAATGCGCCCTAC
PICKLE-LIKE reverse	ACTCTTTCTCAGGTACCCAAGTGC
GH17_39 forward	AACCTGGGTTCAAGACAACG
GH17_39 reverse	CGCATCTCCAGGGTGTACTT
KIN2- LIKE forward	CTGACAATACCCAGAAG
KIN2- LIKE reverse	CTGAGACATCACCTGTT